

ON MINERALS ASSOCIATED WITH ULTRABASIC ROCKS, FOUND IN THE VICINITY OF COMMON BOUNDARIES OF SHIMANE, TOTTORI, OKAYAMA AND HIROSHIMA PREFECTURES (II)

—HYDROPHLOGOPITE AND VARI-GEDRITE FROM THE WAKAMATSU CHROMITE MINE, TOTTORI PREFECTURE—

By

Jun-ichi KITAHARA

Department of Earth Science, Shimane University

Preface

Wakamatsu mine is situated at Tari, Nichinan-machi, Hino-gun, Tottori Prefecture, and has been known as the mine producing chromite ore in ultrabasic rock. Various minerals are found in the chromite deposits, and the author wishes to describe a little about hydrophlogopite and vari-gedrite in this paper.

Outlines of General Geology and Ore Deposits

Ultrabasic rock is intruded into Paleozoic formation, and granitic rock is intruded into the ultrabasic rock. Gabbro and diorite are intruded as dyke and sheet into the ultrabasic rock.

The author has been stated that the basic rock is not a segregated vein from the ultrabasic rock, and they are derived from different mother magmas. The geological area map of the mine has been published in Joun. Jap. Asso. Min. Petro. and Econ. Geol. (1958), and in Sci. Rep. Shimane Univ. (1957).

Chromite ores are segregated from chrome-bearing ultrabasic rock magma, and some of them are intruded into the ultrabasic rock mass. The 7th deposit is operated now, and contains 7th, south and chūgiri levels. These levels are connected each others. Hydrophlogopite and vari-gedrite occurred in the chūgiri level. The chūgiri level is the undermost one in the deposit. The strike and dip of the deposit is N 10° E and 30°-40° W respectively. The deposit is 45 m in length and 40 m in width.

Emplacement of the Chromite-bearing Serpentinite

Paleozoic sediments are intruded by granitic, and ultramafic igneous rocks. Most of the

ultramafic rocks, originally peridotite, pyroxenite, and dunite, have been partly or completely altered to serpentinite or chloritite; they are all designated by the general term serpentinite. The ultrabasics include altered peridotites, serpentinites, harzburgites, altered saxonites, and chromitites (Fig. 1). They are intruded in places by dioritic and gabbroic sills or dykes. The ultrabasic rocks have a regional northwest trend and are



Fig. 1. Photomicrograph showing chromitite composed of olivine, enstatite and chromite (black)
Crossed nicols, $\times 40$
7th deposit of Wakamatsu mine, Tottori pref.

distinguished from the dioritic and gabbroic rocks. In the field it is difficult to separate the different rock units as they grade into one another and sharp boundaries are not commonly observed. The ultrabasic body mainly composed of feldspar free peridotite or harzburgite has been partially serpentinized with subordinate amounts of dunite and pyroxenite. Feldspar in the ultrabasic rocks, if present at all, is a very minor component. Serpentinized peridotite or harzburgite is the dominant ultramafic rock type and comprises about two-thirds of the intrusion; the remainder is dunite and small amounts of enstatite pyroxenite. The subordinate dunite and pyroxenite sometimes occur as thin layer and small irregular masses. Accessory chromite is commonly present in the serpentinite, and some peridotite contains minor diopside augite. Enstatite is everywhere more altered than adjacent olivine and locally is replaced by talc as well as by serpentine or chlorite. Most of the plutonic rocks are probably late Jurassic in age, with ultramafic preceding granitic intrusion. The bodies of serpentinite are commonly elongated parallel to the northwesterly trend as mentioned above and are conformable with the enclosing rocks. These ultrabasic rocks present a striking example of the magmatic differentiation of a slowly cooling ultrabasic magma leading to the development of a great variety of ultrabasic rocks. Veins of steatitized or chloritized pyroxenite and microgabbro locally penetrate the serpentinized peridotite; microgabbro transect the orebody. It is clear that large volume of granitic rocks cannot be expected from the fractionation of magmas of basic composition. The main metamorphic effect resulting from intrusion of the granitic rocks was an increase in serpentinization of adjacent ultramafic rocks.

At stage of the emplacement of the ultrabasics, two immiscible liquids, one chromite rich and the other chromite poor, were co-existent, and are separated into the two liquids. The chromite occurs, generally, in bodies of rather irregular shape, but some are sheet-like and lensoid. The chromite bodies have a regional trend. The structural types of lenses and bands of coarsely crystalline chromite in serpentinite suggest that the segregation was by gravity setting of the chromite crystals while the banding may have developed by magmatic flow. Both high grade massive chromite and lower grade

disseminated chromite occur in very irregular and unpredictable form in serpentinite. During the period of deformation shear fractures, joints and microfractures were developed in chromite crystals and were subsequently filled with the silicate residue of the mineralizers (Fig. 2), which also penetrated into weaker zones of the wall rock. Post mineral

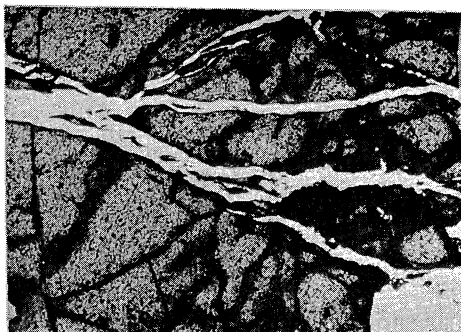


Fig. 2. Photomicrograph showing silicate fluid filled chromite fissures.

Open nicol, $\times 40$

7th deposit of Wakamatsu mine, Tottori pref.

veins of steatitized or chloritized pyroxenite in the rock belong to this period of rock formation, but the unaltered microgabbro veins or dykes probably represent the products of basaltic or gabbroic magma. Dunites, pyroxenites and peridotites during the early stage of magmatic differentiation, are followed by the development of basic rocks. The crystallization of chromite was almost continuous throughout these early stages, but its quantity gradually decreased to scarcity in the pyroxenite members of the group. Contemporaneous with rock consolidation volatile components acted chiefly as mineralizing agents concentrating and subtracting chromium-rich material from the silicate phase. Wall rock is replaced by injection of the ore-forming fluids. Study of thin sections of the wall rocks shows that the introduced chromite corroded and replaced the silicates and moulded itself upon their crystal boundaries. This chromite is clearly distinct from the accessory chromite that formed with the rock-forming silicates during the early stages of magmatic differentiation. Since the effects of hydrothermal alterations are most pronounced within and close to the ore deposits, it is believed that the hydrothermal solutions were set free after the deposition of the chromite. The ore bodies were formed by the injection of residual chromite rich fluids that separated from the differentiated mass of an originally homogeneous magma. The ore constituents and accompanying mineralizers are derived from a common magmatic source. The chromite deposits are regarded as replacement deposits formed by the injection of residual ore-forming fluids that separated from an early-crystallized silicate phase at a late stage in the differentiation of the ultrabasic magma. During the early magmatic period small quantities of chromite crystallized with the silicates, but most of it was kept in a molten state by volatile components, including water and CO_2 , until after the rocks of the orthomagmatic stage had solidified. The chromite injected into wall rocks of the ore deposits is clearly distinguished from early formed accessory chromite as mentioned above. It is highly probable that the hydrothermal solution bearing chromite fluid originated in the ultrabasic magma. The intrusive nature of the deposits, the presence of ore apophyses branching from the main masses into the surrounding rocks, and the clear evidence of wall rock replacement indicates that the ore bodies were formed by the introduction of

an end phase chromite rich differentiated fraction of the parent ultrabasic magma.

Serpentinized Harzburgite (No. 1)

This rock is contacted with diorite dyke, but hydrophlogopite and gedrite are not found there. Under microscope, it is observed that olivine is serpentinized and enstatite is chloritized. Chrome-bearing magnetite or ilmenite is also recognized. Some of enstatite are altered into epidote and titanite by the intrusion of diorite.

The chemical composition of the rock is shown in No. 1, Table 1.

Dioritic Rocks

Diorite, gabbro and feldspathic dykes are widely distributed within the ultramafic intrusion, but are not found in the surrounding paleozoic sediments and granitic rocks. Locally the ultrabasics are cut by dykes of gabbro and diorite.

Diorite Porphyry (No. 4)

The rock occurs in the central part of diorite dyke, and is hard and melanocratic. Under microscope, it is observed that it consists of plagioclase as phenocryst, and plagioclase and hornblende as groundmass, and that they are all relatively fresh. A little amount of biotite is found too. The amount of plagioclase (0.1–0.3 mm) of groundmass is more abundant than that (2.0 mm, idiomorphic-hypidiomorphic) of phenocryst. The content ratio of plagioclase/hornblende is 5/3. It is realized that the plagioclase is andesine, because its cleavage face (001) is almost parallel to the twinning plane. Hornblende in groundmass shows, X' =pale yellow, Z' =yellow. Magnetite is 0.1–0.2 mm in size. Apatite is found too.

The chemical analysis of the rock is shown in No. 4, Table 1.

Diorite (No. 5)

It is melanocratic and hard. Under microscope, plagioclase is 0.2–1.0 mm in size, and forms pericline twin. Its twinning plane \wedge cleavage (001) is 0.5° – 0.6° , so it corresponds to andesine. Hornblende is hypidiomorphic, 0.1–0.2 mm in size, and two types of pleochroism (type I : X' =pale green, Z' =green. type II : X' =pale brown, Z' =brown). Hornblende of 0.02–0.03 mm in size is found too. Little magnetite and ilmenite are observed.

The chemical analysis of the rock is shown in No. 5, Table 1.

Diorite or Diorite Porphyry (No. 7)

This rock is found at the margin of a diorite dyke, and is melanocratic. Under microscope, both groundmass plagioclase of 0.2 mm size and phenocryst plagioclase of 1.5 mm size are recognized. Hornblende shows pleochroism of X' =pale yellow, Z' =green, and its $c \wedge Z' = 17.4^\circ$. Plagioclase is affected by metamorphism, and some of them alter into sericite and the others alter into epidote. The content ratio of plagioclase/hornblende is 5/3.

The chemical analysis of the rock is shown in No. 7, Table 1.

From the value of the chemical analyses (Table 1) and the observation under microscope, it can be found that the margin of a diorite dyke is more acidic and highly altered

than the central part of the dyke.

Table 1. Chemical Compositions of Rocks

No.	Wt. %				Atom. ratios when O=160				
	1	4	5	7	1	4	5	7	
SiO ₂	33.93	56.19	59.24	57.44	Si	30.6	51.5	54.3	51.8
TiO ₂	1.34	0.77	0.83	0.90	Ti	0.9	0.6	0.6	0.6
Al ₂ O ₃	12.78	20.77	18.20	21.26	Al	13.5	22.4	19.6	22.5
Fe ₂ O ₃	2.87	1.93	1.00	1.69	Fe ³	1.9	1.3	0.7	1.2
FeO	3.11	3.54	3.35	1.71	Fe ²	2.3	2.7	2.6	1.3
MnO	0.06	0.05	0.05	0.04	Mn	0.04	0.05	0.06	0.05
MgO	26.23	2.44	3.01	2.95	Mg	35.5	3.4	4.1	4.0
CaO	5.06	7.85	7.53	6.93	Ca	4.9	7.7	7.4	6.7
K ₂ O	0.11	2.21	2.18	2.04	K	0.1	2.6	2.5	2.4
Na ₂ O	0.00	3.90	2.83	3.72	Na	0	6.9	5.1	6.5
P ₂ O ₅	0.06	0.10	0.13	0.09	P	0.05	0.1	0.1	0.1
H ₂ O ₊	10.23	0.36	0.69	0.94	H ₊	61.5	2.2	4.2	5.6
H ₂ O ₋	3.62	0.17	0.22	0.56					
Total	99.40	100.09	100.26	100.27					
		G=2.78							

No.1 : Serpentinized harzburgite, Chūgiri level of 7th deposits of Wakamatsu mine.

Nos. 4, 5, and 7 : Diorite or diorite porphyry, Chūgiri level of 7th deposits of Wakamatsu mine.

(Analyst : J. Kitahara)

Mode of Occurrence of Hydrophlogopite and Vari-Gedrite Associated with the Chromite Deposits

As described above, hydrophlogopite and vari-gedrite are found in chūgiri level of 7th deposits of Wakamatsu mine. Hornblende diorite was intruded along joint or fracture in harzburgite, and reaction between harzburgite and hornblende diorite fluid progressively produced a zoned specific reaction sequence from core of granular serpentine or chlorite through talc-gedrite to hydrophlogopite. At the contact, there is a zone in thickness a few meters, containing mainly hydrophlogopite and anthophyllitic mineral. The formation of the minerals resulted in the desilication of the hornblende diorite fluid. The hydrophlogopite and gedrite specimens were principally taken in the middle of their respective zones, which are virtually monomineralic. The reaction between the dioritic fluid and harzburgite produced a serpentine next to the unaltered olivine and hydrophlogopite next to the serpentine, and the other hand produced a chlorite next to the unaltered enstatite and gedrite next to the chlorite adjacent to the anamorphosed or desilicated hornblende diorite. A zone of gedrite is produced between the hydrophlogopite and diorite. The hydrophlogopite zone does not lie in direct contact with the diorite but is separated from it by the gedrite zone. The contact of the hydrophlogopite and gedrite is rather sharp (Fig. 3). The mode of origin of the hydrophlogopite is of interest in that it appears to be produced from a harzburgite by hydrothermal alteration, due to intrusion of a diorite

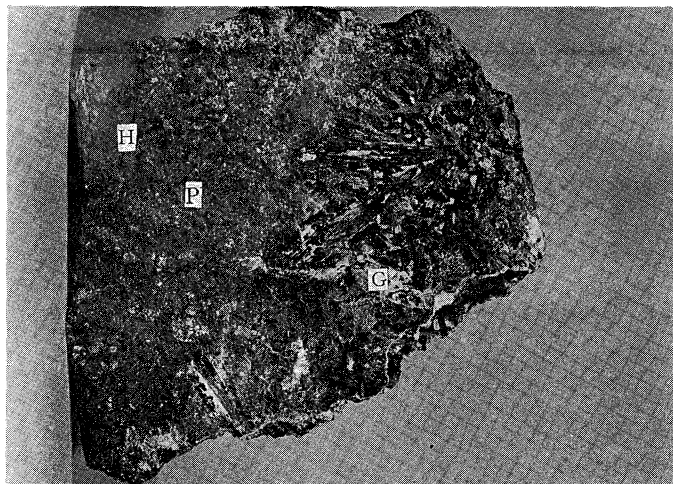
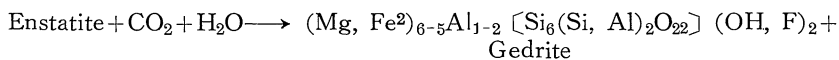
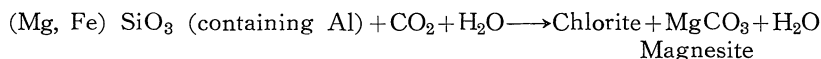
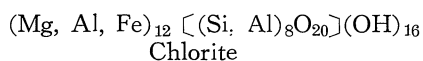
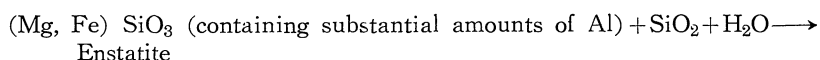


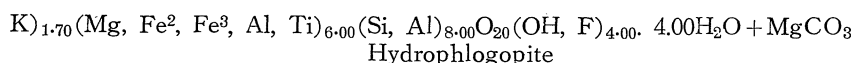
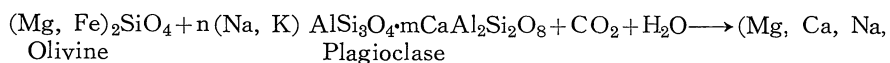
Fig. 3. Photograph showing hydrophlogopite (P) and gedrite (G) in serpentinized harzburgite (in part) (H) side. About $\times 1/2$. Chūgiri level of 7th deposits of Wakamatsu mine.

sheet. The hydrophlogopite appears at a contact zone between a thick diorite and harzburgite. The thickness of this hydrophlogopite varies between 0.5 m and 2 m. The gedrite occurs as a replacement of ultrabasic rock particularly harzburgite. In these bodies the gedrite assumes its own characteristic form in replacement the chlorite altered from enstatite. The alteration of enstatite to chlorite involves either the addition of silica and water or the removal of magnesia by solutions carrying CO_2 as the following chemical change.



Magnesite does not occur as a product in this stage. The magmatic solutions from dioritic intrusive penetrate through the ultrabasic rock and replace the chlorite altered from enstatite by a gedrite. The solutions in early stages were mainly siliceous, and they penetrated the harzburgite bodies change the enstatite to chlorite and to gedrite.

The hydrophlogopite is in the region of contact between intrusive diorite and ultrabasic rock such as harzburgite. In these circumstances it is found associated with apatite, serpentine, chlorite and talc. The hydrophlogopite is in most cases produced hydrothermally, and not by weathering, and occurs with apatite in the harzburgite. The origin of the hydrophlogopite is probably derived by a hydrothermal contact metasomatic replacement of harzburgite associated with the introduction of F, P, Ti and CO_2 .



Ferrous iron is oxidized, $(\text{OH})^{-1}$ replace O^{-2} , and magnesium is lost, but the flakes remain physically stable.

The hydrophlogopite and gedrite occur in close association with chloritized pyroxene and/or serpentinized olivine, not only in alone the wall of the diorite dyke. The hydrophlogopite is occasionally found in disseminated form within the harzburgite mass (Fig. 4). The disseminated hydrophlogopite is typical of mineral that have been formed by

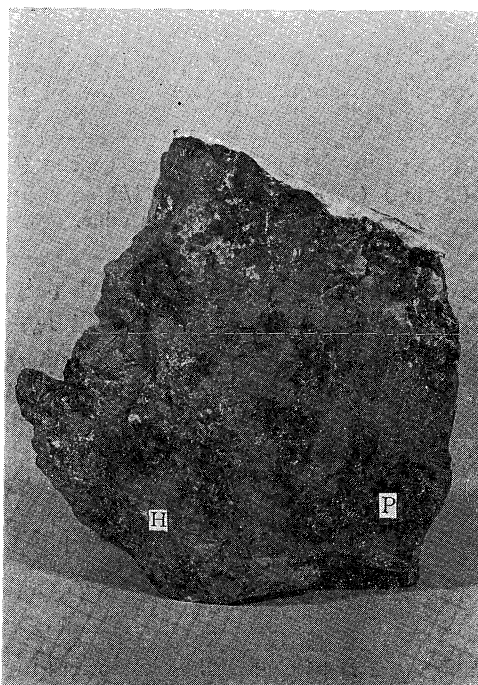


Fig. 4. Photograph showing disseminated hydrophlogopite (P) in serpentinized harzburgite (H). About $\times 3/5$. Chūgiri level of 7th deposits of Wakamatsu mine.

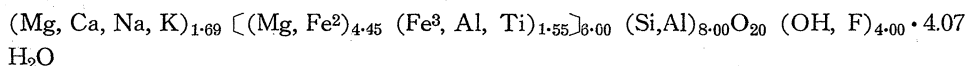
hydrothermal process. The hydrophlogopite is a Mg-Al rich mineral, and the gedrite is a Mg-Al-Si rich mineral. Both require a Mg-Al and Mg-Al-Si sources respectively. These can be provided by reaction of the harzburgite and hornblende diorite as described before. Both are a Mg-Al rich mineral and are possibly derived from ultrabasic parent through the addition of hornblende diorite material. It is regarded the hydrophlogopite and gedrite are the products of hydrothermal metamorphism related to igneous emanations. The writer believes that these solutions which caused the alteration, were emanations from dioritic rock, and that the solutions were hot, alkaline and were at first siliceous and carried some aluminium in addition to magnesium, later becoming less siliceous, poor in magnesium and rich in aluminium. Perhaps the hydrothermal metamorphism or alteration is much like the contact metamorphism and is related to igneous emanations.

brownish or reddish colour. MgO thins or hides the colour produced by TiO₂. The γ colour of phlogopite (FeO 10.12, Fe₂O₃ 3.96, TiO₂ 1.95, MgO 15.21 wt%), which resembles to hydrophlogopite of this mine in chemical composition, is brownish yellow. When it contains more MgO or H₂O like the hydrophlogopite of this mine, its γ colour fades and becomes pale brownish yellow or pale yellow. On the other hand, its TiO₂ content is as little as 0.73%, so, γ colour shows pale green to pale yellow. $\Sigma\text{FeO} = (\text{FeO} + \text{Fe}_2\text{O}_3 = 10.04\%)$ content add brownish tone to γ colour. It can be considered that, its γ colour will become pale brownish yellow finally.

Chemical Composition of Hydrophlogopite

As described above, hydrophlogopite and gedrite occur in different zones, so, hydrophlogopite is able to pick up separately. The result of chemical analysis of hydrophlogopite is shown in Table 2.

As shown in Table 2, it is more just to call this mineral as hydrophlogopite than to call it as hydrobiotite, because of its high MgO content. The analysis contains considerable amounts of alkalis. The chemical formula obtained from the chemical analysis data is as follows.



The ideal formula for the hydrophlogopite would be $(\text{OH})_4\text{K}(\text{Mg, Fe})_8(\text{Si, Al, Fe})_8\text{O}_{20} \cdot 4\text{H}_2\text{O}$. Al replaces Si in tetrahedral sites usually beyond the ratio Al/Si=2/6. From this formula, it is resolved that the hydrophlogopite corresponds to a mineral which has medium chemical composition between phlogopite and vermiculite which is alteration

Table 2. Chemical Composition of Hydrophlogopite

	Wt. %	Mols	Atom. Ratios		Ditto when O=22
SiO ₂	34.35	573	Si	573	5.392
TiO ₂	0.73	9	Ti	9	0.084
Al ₂ O ₃	19.80	194	Al	388	3.651
Fe ₂ O ₃	3.62	23	Fe ³	46	0.433
FeO	6.78	94	Fe ²	94	0.885
MnO	0.06	1	Mn	1	0.009
MgO	19.00	475	Mg	475	4.470
CaO	0.52	9	Ca	9	0.084
Na ₂ O	0.13	2	Na	4	0.035
K ₂ O	3.25	35	K	70	0.659
F	0.14	7	F	7	0.066
H ₂ O ₊	6.37	354	H ₊	708	OH ₊ - 12.063
H ₂ O ₋	5.17	287	H ₋	574	
	99.92				
O≡F	0.06				
Total	99.86				

(Analyst : J. Kitahara)

product of the former by hydration. Further from the constitutional formula of mica, it can be said that, the ratio $\Sigma\text{FeO} = (\text{FeO} + \text{Fe}_2\text{O}_3)/\text{MgO} = 0.50 - 1.52$, and that $\text{Fe}_2\text{O}_3/\text{FeO} = 0.14 - 0.28$. The values FeO/MgO and $\text{Fe}_2\text{O}_3/\text{FeO}$ of the hydrophlogopite of this mine are 0.528 and 0.534 respectively. The fact that the $\text{Fe}_2\text{O}_3/\text{FeO}$ value is higher than that of mica, is due to the alteration of phlogopite into hydrophlogopite. Hydrophlogopite have higher content of $[\text{Al}]^4$ than the coexisting gedrite. As described above, this alteration occurred according to the order of olivine \rightarrow serpentine \rightarrow hydrophlogopite, and hydrophlogopite is a primary mineral generated in later stage. In igneous rocks the iron content of biotite or phlogopite increases with SiO_2 content of the rock, ultrabasic rocks containing phlogopite, granites and granite pegmatites containing iron-rich biotite. When the chemical composition of hydrophlogopite is plotted, without consideration of water content, in Engel's chemical composition diagram of biotite-phlogopite system which is determined by rock type, the hydrophlogopite comes into the area of ultrabasic rock. The Engel's diagram is made by rearrangement of Heinrich's diagram.

X-Ray Diffraction Data by Powder Method of Hydrophlogopite

The author took a x-ray photograph of the hydrophlogopite under following conditions, Copper K_α radiation (3.5 kV, 15 mA) was used. The radius of the camera was 45.02 mm, the powder specimen was cylindrical with a diameter not exceeding 0.3 mm, and was constantly rotated during the exposure in order to secure uniform intensities of diffraction lines. Exposure times were approximately 3.5 hrs. The intensities of the lines were estimated visually. The result is shown in Table 3. The results obtained by recording x-ray diffractometer are shown in Fig. 5 and the table. The sample is fine powder, and the instrumental conditions are as follows.

X-ray	35 kVp,	15 mA (Cu- K_α radiation)
Full scale		1000 C. P. S.
Scanning speed		1°/min.
Chart speed		10 mm/min.
Time constant		1.25 second.
R. slit		0.2 mm.
D. slit		2.0 mm.

The x-ray data in the table show clearly that the mineral is made up of interstratified layers of units of mica and vermiculite, and d-value 1.415 is due to the reflection on (0. 0. 20) face of vermiculite, and d-value 3.278 is due to the reflection on (006) face of mica. So, hydrophlogopite consists of mixed layer of phlogopite and vermiculite, and its calculated d-value (001) is 24.1 Å. The mineral contains alkalis to an appreciable extent, so a type of mineral results which is neither a vermiculite nor a mica but an "interstratification" unit layers of these two. In hydrophlogopite or hydrobiotite, potassium intersilicate layers alternate with intersilicate layers containing bivalent ions and water molecules. The stacking along c axis of the hydrophlogopite is a regular repetition of the different layers. In such cases, the resulting structure has distinctive characteristics; the unit cell is equivalent to the sum of the component layers, and regular (001) reflections are obtained. In the case of the hydrophlogopite which is a regular interstratification

Table 3. X-Ray Powder Diagrams of Hydrophlogopite taken with Copper K_{α} Radiation

Photograph		Recorder		hkl (indices)
d	I	d	I/I ₁	
		14.488	59	002 V
		10.163	95	002 m
		7.314	39	
		4.901	38	
		4.171	33	
		3.619	47	008 V
		3.480	55	
		3.376	100	007 or 0.0.18 h
3.278	m	3.314	39	006 m
		3.209	39	
		3.175	38	
		3.153	39	
2.867	w	2.894	40	0.0.10 V
2.592	m	2.629	40	
		2.522	39	m
2.436	w	2.442	38	
		2.276	31	
		2.186	34	
		2.062	31	
		2.040	37	
		2.023	39	
2.002	ms	2.019	41	
		2.002	33	
1.859	f	1.922	30	
		1.713	31	
1.670	s or b	1.681	37	
1.533	s	1.537	36	060 and others
1.425	w	1.443	33	
1.351	ms	1.370	32	
1.274	f			

V : reflection of vermiculite, h : reflection of hydrophlogopite,
m : reflection of mica.

of phlogopite and vermiculite, the diffraction effect is equivalent to a unit cell which is a multiple of the individual layers. Hydrophlogopite may be looked upon as ordinary phlogopite interleaved with vermiculite containing replaceable Mg and Ca ions. The position and intensity of the composite reflections will vary with the relative abundance of the different individual layers. It may as in specimen approach a definite ratio of 1/1=phlogopite/vermiculite units. Further, from the chemical analysis data shown in Table 2, it is considered that hydrophlogopite consists of a regular mixed layer of phlogopite and vermiculite.

On the other hand, because d-value 3.376 is due to the reflection on (007) face of

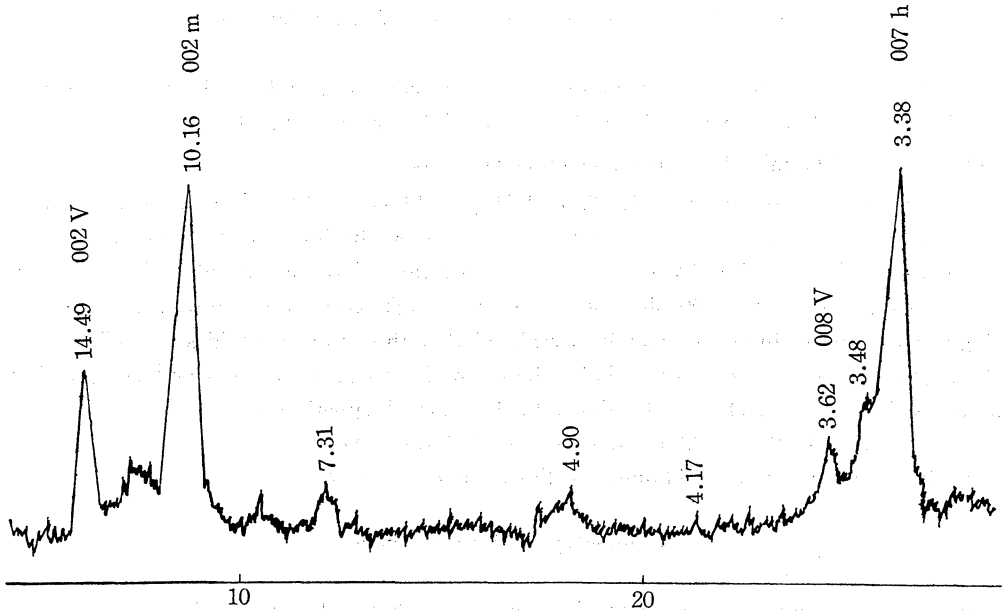


Fig. 5. X-ray diffraction chart of hydrophlogopite at low 2θ angles.

hydrophlogopite, its d-value (001) is calculated as 23.6 Å. Then its mean d-value (001) is 23.9 Å. D-value 2.173 of phlogopite shows strong reflection, but that of hydrophlogopite is not present. This is remarkable difference between them. Moreover, the face corresponding to d-value 3.278 does not exist in vermiculite, but it is recognized in hydrophlogopite or hydrobiotite. X-ray diagrams are necessary to distinguish vermiculite from hydrophlogopite. The c parameter of phlogopite decreases as iron content increases although the ionic radius of Fe^{2+} is greater than that of Mg^{2+} . It is assumed that this spparent anomaly is due to the greater polarising power of Fe^{2+} ions.

Paragenesis of Hydrophlogopite

From the chemical analysis data table 2, its stomic and molecular ratios can be expressed as follows.

$$[\text{Si}]^4 : 5.39, [\text{Al}]^4 : 2.61, [\text{Al}]^6 : 1.04, \Sigma\text{FeO} = (\text{FeO} + \text{Fe}_2\text{O}_3)/\text{MgO} : 0.53,$$

$$\text{Fe}_2\text{O}_3/\text{FeO} : 0.53, \text{MnO} : 0.06, \text{Na}_2\text{O}/\text{K}_2\text{O} : 0.04.$$

These values represent a grade of hydrophlogopite producing reaction between pyroxene peridotite and hornblende diorite. These values show that, hydrophlogopite is paragenetic with pyroxene or olivine or both of them, but not paragenetic with gedrite of amphibole group. Diorite dyke is intruded into pyroxene peridotite and produced hydrophlogopite in the latter side. So, it can be said that hydrophlogopite is paragenetic with both pyroxene and olivine. As described above, as hydrophlogopite and gedrite show zonal occurrence, they may be considered as if paragenetic. But it can not be said that they are paragenetic, because they do not accompany so closely.

Physical and Chemical Properties of Vari-Gedrite

The vari-gedrite forms blackish prisms about one cm long, with tendency of aggregation. Its black colour is caused by Fe^3 content (Fe^3 is richer than Fe^2).

The density determined by pycnometer is $D_4^{19}=3.037$.

The optical properties are : $\alpha=1.633$, $\beta=1.645$, $\gamma=1.653$. $(-)2V=78.8^\circ$. In thin section, X' = pale green, Z' = green. Indices were determined by the immersion method.

The relation between $\text{Mg}/(\text{Mg}+\text{Fe}^2+\text{Fe}^3+\text{Mn})$ ratio and refractive index of the mineral is shown in diagram. The 100 $\text{Mg}/(\text{Mg}+\text{Fe}^2+\text{Fe}^3+\text{Mn})$ ratio is 85.9, so from the diagram (diagram is omitted in the paper) it is realized that the index coincides to 1.651.

Hey (1956) has expressed the relation between the refractive indices and composition on the basis of 24 (O, OH, F) by the following partial equation :

$$\gamma=1.7249-0.0130\text{Si}+0.0140(\text{Ti}+\text{Fe}^3+\text{Fe}^2+\text{Mn})$$

The γ index of the sample obtained by the equation is 1.666.

Chemistry of Vari-Cedrite

The main variations in the composition of the anthophyllite and gedrite minerals are related to the substitutions $\text{Mg} \rightleftharpoons \text{Fe}^2$ and $(\text{Mg}, \text{Fe}^2) \text{Si} \rightleftharpoons \text{AlAl}$, and these orthorhombic amphiboles can be expressed in terms of the four endmember composition, anthophyllite $\text{Mg}_7\text{Si}_8\text{O}_{22}(\text{OH})_2$, ferroanthophyllite $\text{Fe}_7^2\text{Si}_8\text{O}_{22}(\text{OH})_2$, gedrite $\text{Mg}_5\text{Al}_4\text{Si}_6\text{O}_{22}(\text{OH})_2$, and ferrogedrite $\text{Fe}_5^2\text{Al}_4\text{Si}_6\text{O}_{22}(\text{OH})_2$. Gedrite close in composition to $\text{Mg}_5\text{Al}_4\text{Si}_6\text{O}_{22}(\text{OH})_2$ have not been reported. Most orthorhombic amphiboles are either poor in aluminum ($<0.5[\text{Al}]^4$) or rich in aluminum ($>1.5[\text{Al}]^4$ per formula unit), and it is probable that there is a continuous solid solution series between $\text{Mg}_7\text{Si}_8\text{O}_{22}(\text{OH})_2$ and $\text{Fe}_5^2\text{Al}_4\text{Si}_6\text{O}_{22}(\text{OH})_2$. The variation of Si and Al appears to reflect several factors, increased substitution of Al for Si with rising temperature.

The vari-gedrite was separated from its host rock and hydrophlogopite, by hand tapping. The material thus obtained was analysed. The chemical composition and atomic ratios of the specimen are shown in Table 4. From the table, it is seen that the sample contains high Al_2O_3 .

The general formula of anthophyllite is $\text{X}_7\text{Y}_8\text{O}_{22}(\text{OH}, \text{F})$. In X the maximum amount of Al is $(\text{Mg}, \text{Fe}^2)_5\text{Al}_2$, and the maximum amount of Fe^2 is about $(\text{Mg}_{3.5}, \text{Fe}_{3.5})$. In Y the maximum amount of Al is (Si_6Al_2) . Gedrite is an aluminian variety of anthophyllite. The formula for gedrite is $(\text{Mg}, \text{Fe}, \text{Al})_7(\text{Al}, \text{Si})_8\text{O}_{22}(\text{OH})_2$. It should be emphasized that by this scheme Al can replace Si up to a limit of 2 atoms and it can replace Mg and Fe also up to a limit of 2 atoms. The formula for such a maximum replacement would be $(\text{Mg}, \text{Fe})_5\text{Al}_2(\text{Si}_6\text{Al}_2)\text{O}_{22}(\text{OH})_2$. Also, OH can be replaced by F. Some varieties are highly aluminous, the aluminium may be present as $\text{MgAl}_2\text{SiO}_6$.

In the calculation of the formula, on the basis of 24(O, OH, F) and 8(Si, Al) as shown in the table, the examination of (Ca, Mg, K, Fe^2 , Fe^3 , Mn, Ti, Al) must be 7 ± 0.5 . This figure will be called X.

Silica in the anthophyllite series ranges from 42.18% to 60.13%. This nearly covers the theoretical limits of 38.25–61.70%. Naturally, with increasing iron and aluminum, silicon

decreases, the greatest decrease coinciding with increase in aluminum. Titanium seems to go with either aluminum or iron or both.

Table 4. Chemical Analysis of Vari-Gedrite

	Wt. %	Mols	Atom. ratios		Atom. ratios when (O,OH,F,(Cl)) = 24
SiO ₂	40.38	673	Si	673	5.438
TiO ₂	1.11	14	Ti	14	0.113
Al ₂ O ₃	30.89	303	Al	606	4.897
Fe ₂ O ₃	3.71	23	Fe ³	46	0.372
FeO	1.85	26	Fe ²	26	0.210
MgO	17.53	438	Mg	438	3.539
CaO	0.51	9	Ca	9	0.073
MnO	0.00	0	Mn	0	0.00
Na ₂ O	1.02	17	Na	34	0.275
K ₂ O	0.13	1	K	2	0.016
H ₂ O ₊	2.22	123	(H ₊),OH	246	1.988
H ₂ O ₋	0.22				
F	0.06	3	F	3	0.024
	99.63				
O≡F,(Cl)	0.06	4			
	99.57				

Numbers of ions on basis of 24(O, OH, F, Cl)

Si	5.438	} 8.00
Al	2.562	
Al	2.335	} 6.993
Ti	0.113	
Fe ³	0.372	
Mg	3.539	
Fe ²	0.210	
Mn	0.0	
Na	0.275	
Ca	0.073	} 2.012
K	0.016	
OH	1.988	
F	0.024	

(Analyst : J. Kitahara)

X-Ray Powder Data for Vari-Gedrite

X-ray photograph of gedrite was taken in a camera of 90.04 mm diameter, using Cu K_α (1.5418) radiation. The voltage used is 35 kVp at 15 mA, and the exposure time was nearly 1.5 hours. The record of the x-ray diffraction on photographic film was attempted by the method of Bradley and Jay. The x-ray powder lines for the specimen were indexed and given in Table 5.

On the other hand, the data of the gedrite sample showed by the recording x-ray

Table 5. X-Ray Powder Data for Vari-Gedrite

Photograph		Recorder		hkl(indices)
d	I	d	I/I ₁	
		8.37	29	210
		6.34	54	
		4.94	50	230, 101, 011, 111
		4.56	35	400
4.114	w	4.18	71	420, 301
		3.94	69	301
3.414	ms	3.43	100	421, 440, 150
		3.34	34	331
		3.08	27	610, 501
		2.97	30	
2.894	s	2.91	93	521
		2.86	27	260, 450
		2.57	26	112, 621, 640
2.522	s	2.53	83	460, 202, 541, 022
2.374	w(m)	2.35	42	650, 170, 730
		2.33	32	551
		2.29	34	461, 412, 042
		2.14	30	502
2.103	w(m)	2.12	30	561
		2.09	29	
		2.08	29	840
		2.01	37	661
2.014	sm	1.99	54	480, 281, 532
		1.97	25	751
1.899	m(w)	1.87	40	702, 10.0.0, 761, 191, 712
		1.83	24	931
		1.81	23	
1.734	f	1.73	24	391, 921, 490, 880, 10.3.0, 530
1.631	m	1.61	35	880, 912, 2.11.0
		1.59	25	11.0.1, 423
1.575	mw	1.55	30	12.0.0
		1.54	24	
		1.48	24	12.3.0, 0.12.0, 623, 10.2.2
1.480	mw	1.46	30	
		1.43	21	
		1.42	24	
1.441	mw	1.41	29	703, 10.3.2, 592, 2.12.0, 2.10.2, 12.2.1
		1.38	25	
1.395	m	1.36	29	13.0.0, 12.5.0, 10.8.0, 980
1.321	wf	1.31	21	
1.299	mw	1.28	9	882
		1.26	9	
1.258	m	1.22	8	2.12.2, 13.5.1, 14.0.1

diffractometer are denoted in Fig. 6 and the same table. The sample is fine powder, and the instrumental conditions are all the same as the determination of hydrophlogopite mentioned already.

Relation of spacings to cell geometry is given as the following equation.

$$\frac{1}{d_{hkl}^2} = \frac{h^2 b^2 c^2 \sin^2 \alpha}{V^2} + \frac{k^2 a^2 c^2 \sin^2 \beta}{V^2} + \frac{l^2 a^2 b^2 \sin^2 \gamma}{V^2} \\ + 2hk \frac{abc^2}{V^2} (\cos \alpha \cos \beta - \cos \gamma) \\ + 2kl \frac{a^2 bc}{V^2} (\cos \beta \cos \gamma - \cos \alpha) \\ + 2lh \frac{ab^2 c}{V^2} (\cos \gamma \cos \alpha - \cos \beta),$$

where $V = abc \sqrt{1 - \cos^2 \alpha - \cos^2 \beta - \cos^2 \gamma + 2 \cos \alpha \cos \beta \cos \gamma}$.

The reduction for orthorhombic system becomes as the next equation.

$$\frac{1}{d_{hkl}^2} = \frac{h^2}{a^2} + \frac{k^2}{b^2} + \frac{l^2}{c^2}.$$

The spacing as a function of cell edges is calculated from the above equation. The cell edges, therefore, are obtained oppositely from the face indices. The d-value ($d = 1.2578$) of the most outer line of x-ray powder photograph corresponds to face indices ($hkl = 2.12.2, 13.5.1, 14.0.1$). The cell edges (a_0, b_0, c_0) are obtained as the following values from the above mentioned formula, $a_0 = 18.147 \text{ \AA}$, $b_0 = 17.462 \text{ \AA}$, $c_0 = 5.205 \text{ \AA}$

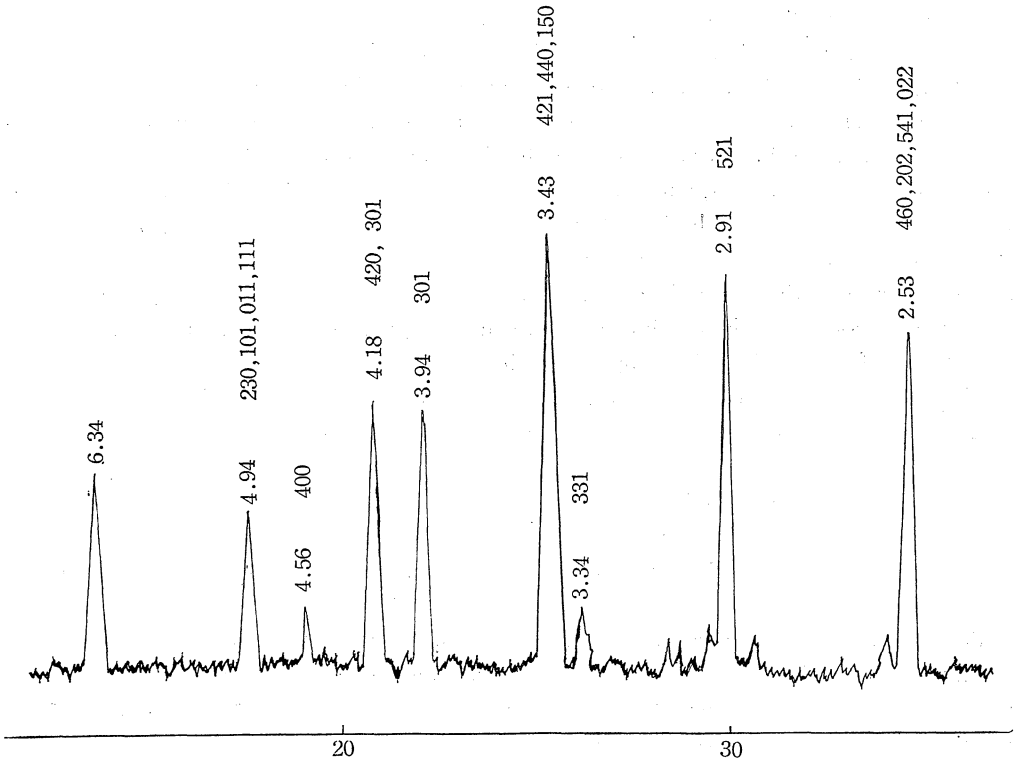


Fig. 6. X-ray diffraction chart of vari-gedrite at low 2θ angles.

Francis and Hey (1956) derived from a number of analysed specimens the relationship $b (\text{Å}) = 16.44 + 0.28\text{Si} - 0.13\text{Mg} + 0.40 (\text{Ca} + \text{Na} + \text{K})$ where Si, Mg, Ca, etc., are numbers of atoms per formula unit on the basis of 24 (O, OH). The standard deviation in b was given as $\pm 0.04 \text{ Å}$. It is seen that b increases with substitution of Fe for Mg and with (Ca, Na, K) content, and decreases with substitution of Al for Si. Many other substitution are possible, so that the above equation may sometimes give a value of b considerably different as follows from that observed.

$$b (\text{Å}) = 16.44 + 0.28 \times 5.438 - 0.13 \times 3.539 + 0.40 \times (0.073 + 0.275 + 0.016) = 17.648$$

Summary and Conclusions

Ultrabasic rocks are invaded by gabbroic rocks in the region. The writer has been described that the ultrabasic and gabbro-dioritic rocks are originated from different magmas. Chromites are segregated from chromium bearing ultrabasic magma and some parts of the chromites are intruded into the ultrabasic rocks.

Hydrophlogopite and vari-gedrite was found by the writer in 1959 in the chūgiri level of 7th deposits of the Wakamatsu mine. These were produced by metasomatic replacement related to igneous emanations caused by the intrusion of hornblende diorite dyke into serpentinized harzburgite contacted with chromite ore. Gedrite preceding to hydrophlogopite is generated. Hydrophlogopite is found contacting with gedrite, but they are not paragenetic each others and occur rather in different zones. Usually hydrophlogopite occurs in harzburgite side and gedrite occurs contacting with diorite. Sometimes both of them occur in diorite side. These occurrence may be caused by the difference of the physico-chemical condition under which the two kind of rocks reacted. Components such as Al_2O_3 , $\text{FeO} + \text{Fe}_2\text{O}_3$ and $\text{K}_2\text{O} + \text{Na}_2\text{O}$ come into harzburgite from diorite, and MgO , CaO components are partly extruded from harzburgite. Then, as described above, hydrophlogopite and gedrite were formed in the harzburgite side of the boundary between these two rocks. Sometimes, when diorite or diorite porphyry are intruded into serpentinized harzburgite, disseminated hydrophlogopite is found in the latter 2 m apart from the boundary of these rocks. Under microscope, it is observed that olivine is altered to serpentine and further to hydrophlogopite, by the effect of hydrothermal liquid derived from diorite dyke which has intruded into harzburgite. On the other hand, such an alteration is found under microscope, enstatite to chlorite and to gedrite.

The chemical formula of the hydrophlogopite is shown in the table. It seems clear that the present mineral is a regular mixed layer type composed of phlogopite and vermiculite. The γ index of the mineral is 1.6051, and the calculated value is 1.604. The lattice constant $d(001)$ is 23.9 Å.

The chemical composition and its atomic ratios of the vari-gedrite are given in the table. The γ index is 1.6533, and the lattice constants are $a_0 = 18.147 \text{ Å}$, $b_0 = 17.462 \text{ Å}$, and $c_0 = 5.205 \text{ Å}$.

The hydrophlogopite and vari-gedrite occur in banded form, but judging from the chemical composition of the hydrophlogopite, it shows that the mineral is not generated with the gedrite and associated with pyroxene and/or olivine. A part of the hydrophlogopite is seen as a disseminated form in serpentinite. Hydrophlogopite and vari-gedrite occurred in an alteration process according to such an order as olivine \rightarrow

serpentine→hydrophlogopite, and enstatite→chlorite→vari-gedrite respectively.

Acknowledgments. The writer wishes to thanks to the head of Wakamatsu mine, Nippon Chrome Kōgyō K. K., Thuneo Nozaka and the mining engineer, Kazuo Kinutani for the writer's survey of the mine. This study was aided by a grant from the Scientific Research of the Department of Education.

References

- Amin, M. S. and Afria, M. S., (1954), Anthophyllite-vermiculite deposit of Hafafit, Eastern Desert, Egypt. *Econ. Geol.*, **49**, p. 317.
- Anderson, A. L., (1931), Genesis of anthophyllite deposits near kamiah, Idaho. *Jour. Geol.*, **39**, p. 68.
- Azaroff, L. V and Buerger, M. J., (1958), "The powder method of x-ray crystallography". McGroW-Hill.
- Bilgrami, S. A., (1964), Mineralogy and petrology of the central part of the Hindubagh igneous complex, Hindubagh mining district, Zhob Valley, West Pakistan. *Rec. Geol. Surv. Pakistan*, X, Part 2-C, p.1.
- Brown, G. and Norrish, K., (1932), Hydrous micas. *Min. Mag.*, **29**, P. 929.
- Chayes, F. A., (1948), A petrographic criterion for the possible replacement origin of rocks. *Am. Jour. Sci.*, **246**, p. 413.
- Deer, W. A., Howie, R. A., and Zussman, J., (1962), (1963), "Rock forming minerals". **2, 3**. Longmans.
- Engel, A. E. J. and Engel, C. G., (1960), Progressive metamorphism and granitization of the Major paragneiss, northwest Adirondack Mountains, New York. Part II, Mineralogy. *Bull. Geol. Soc. Am.*, **71**, p. 1.
- Francis, G. H., (1955), Gedrite from Glen Urquhart, Inverness-shire. *Min. Mag.*, **30**, p. 709.
- and Hey, M. H., (1956), The unit cell contents of anthophyllite. *Min. Mag.*, **31**, p. 173.
- Gruner, J. W., (1934), The structure of vermiculite and their collapse by dehydration. *Am. Min.*, **19**, p. 557.
- Hall, A. J., (1944), The relation between colour and chemical composition in the biotites. *Am. Min.*, **26**, p. 29.
- Harry, W. T., (1950), Aluminum replacing silicon in some silicate lattice. *Min. Mag.*, **29**, P. 142.
- Hayama, Y., (1959), Some consideration on the colour of biotite and its relation to metamorphism. *Jour. Geol. Soc. Japan*, **65**, p. 21.
- Heinrich, E. W., (1946), Studies in the mica group; the biotite phlogopite series. *Am. Jour. Sci.*, **244**, p. 836.
- Hey, M. H., (1956), On the correlation of physical properties with chemical composition in multivalent systems. *Min. Mag.*, **31**, p. 69.
- Katayama, N., (1964), "The earth sciences", a textbook for general education at collages. Iwasaki (in Japanese).
- Kitahara, J., (1957), Studies on the chromites and their country rocks from the Tari district, Tottori Pref. *Sci. Rep. Shimane Univ.*, **7**, p. 77.
- , (1965), Hydrophlogopite from the Wakamatsu chromite mine, Tottori Pref. *Jour. Jap. Assoc. Min. Petr. Econ. Geol.*, **54**, p. 32 (in Japanese).
- Kulp, J. L. and Brobst, D. A., (1954), Notes on the dunite and the geochemistry of vermiculite at the Day Book deposit, Yancey Country, North Carolina. *Econ. Geol.*, **49**, p. 211.
- Kunitz, W., (1924), Die beziehungen zwischen der chemischen znsammensetzung und den physikalisch-optischen eigenschaften innerhalb der glimmergruppe. *Neues Jahrb.*, B1-Bd. **50**, P. 365.
- Nagelschmidt, B., (1937), X-ray investigation on clays, Part 3. *Zeit. Krist.*, **97**, p. 514.

- Nockolds, S. R., (1947), The relation between chemical composition and paragenesis in the biotite micas of igneous rocks. *Am. Jour. Sci.*, **245**, p. 401.
- Ostrovsky, J. A. and Petriv, V. P., (1940), Materials on the relations between optical properties and the chemical composition of ferro-magnesium micas. *Trans. Geol. Inst. Academy Sciences USSR.*, **36**, Petrogr. Ser. No. 2 (in Russian).
- Rabbitt, J. G., (1948), A new study of the anthophyllite series. *Am. Min.*, **33**, p. 263.
- Schwartz, G. M., (1958), Alteration of biotite under mesothermal conditions. *Econ. Geol.*, **53**, p. 164.
- Seki, Y. and Yamasaki, M., (1957), Aluminian ferroanthophyllite from the Kitakami mountain-land, north-eastern Japan. *Am. Min.*, **42**, p. 506.
- Shams, F. A., (1964), Structures in chromite-bearing serpentinite, Hindbagh, Zhob Valley, West Pakistan. *Econ.*, **59**, p. 1343.
- Shibata, H. and Sudo, T., (1964), "Keys to the illustrated manual of minerals and rocks in full colour". *Hokuryūkan* (in Japanese).
- Shimoda, S., (1958), Hydrous complex of mica caly mineral. *Advan. Clay Sci.*, (2), p. 115 (in Japanese).
- Yamada, H. and Sugiura, K., (1940), on the hydrated biotite in Motomiya clay. *Jour. Jap. Assoc. Petr. Econ. Geol.*, **34**, p. 122 (in Japanese).

Manuscript received, September 6, 1965.